

# Pragmatic Approaches to Reducing Radiation Dose in Brain Computed Tomography Scan using Scan Parameter Modification

## Abstract

**Background:** High radiation dose of patients has become a concern in the computed tomography (CT) examinations. The aim of this study is to guide the radiology technician in modifying or optimizing the underlying parameters of the CT scan to reduce the patient radiation dose and produce an acceptable image quality for diagnosis. **Methods:** The body mass measurement device phantom was repeatedly scanned by changing the scan parameters. To analyze the image quality, software-based and observer-based evaluations were employed. To study the effect of scan parameters such as slice thickness and reconstruction filter on image quality and radiation dose, the structural equation modeling was used. **Results:** By changing the reconstruction filter from standard to soft and slice thickness from 2.5 mm to 5 mm, low-contrast resolution did not change significantly. In addition, by increasing the slice thickness and changing the reconstruction filter, the spatial resolution at different radiation conditions did not significantly differ from the standard irradiation conditions ( $P > 0.05$ ). **Conclusion:** In this study, it was shown that in the brain CT scan imaging, the radiation dose was reduced by 30%–50% by increasing the slice thickness or changing the reconstruction filter. It is necessary to adjust the CT scan protocols according to clinical requirements or the special conditions of some patients while maintaining acceptable image quality.

**Keywords:** Multidetector computed tomography scans, radiation dose, scan parameter modifications, software- and observer-based evaluations

Submitted: 29-Dec-2020

Accepted: 01-Nov-2021

Published: 26-Jul-2022

## Introduction

Although computed tomography (CT) produces high-quality and accurate images and is widely used in early medical diagnoses, it can be a relatively high radiation dose imaging modality.<sup>[1]</sup> Increasing CT use has been attributed to its ubiquitous presence, ease of operation, short acquisition time, emerging applications (such as material characterization with dual energy, organ perfusion analysis, and virtual colonoscopy), and positive impact on patient throughput.<sup>[2]</sup> Previous studies have shown that while CT scan accounts for only 15% of all imaging examinations, it accounts for more than 75% of all radiation doses.<sup>[3-5]</sup> For this, the radiology community has paid much attention to reducing the exposure of patients, through the optimization of scanning protocols. To determine the reference dose levels in the different CT studies (e.g. pancreatic protocol, routine

abdominal, and pelvic scan), and make appropriate changes to reduce dose levels, process improvement techniques must be thoroughly understood.<sup>[2]</sup> Low-dose CT imaging has always been difficult because reducing the dose increases the noise and reduces the image's diagnostic quality. To optimize CT examination protocols, a basic understanding of CT scan parameters and their effect on image quality is required. Naturally, the attempts have to make a compromise between patient radiation dose and noise or image quality.

A few studies have optimized image quality and radiation dose by changing the slice thickness and the reconstructed filter.<sup>[6,7]</sup> Most of these studies have either examined the effect of scan parameters on radiation dose and image quality in chest and abdominal and pelvic imaging.<sup>[6-8]</sup>

From another point of view, human decision-making criteria, because of their decisive role in the diagnosis of the disease,

This is an open access journal, and articles are distributed under the terms of the Creative Commons Attribution-NonCommercial-ShareAlike 4.0 License, which allows others to remix, tweak, and build upon the work non-commercially, as long as appropriate credit is given and the new creations are licensed under the identical terms.

For reprints contact: WKHLRPMedknow\_reprints@wolterskluwer.com

**How to cite this article:** Choopani MR, Abedi I, Dalvand F. Pragmatic approaches to reducing radiation dose in brain computed tomography scan using scan parameter modification. *J Med Sign Sens* 2022;12:219-26.

**Mohammad Reza Choopani<sup>1</sup>, Iraj Abedi<sup>2</sup>, Fatemeh Dalvand<sup>3</sup>**

<sup>1</sup>Departments of Radiology, Isfahan University of Medical Sciences, Isfahan, Iran,

<sup>2</sup>Department of Medical Physics, Isfahan University of Medical Sciences, Isfahan, Iran,

<sup>3</sup>Department of Medical Radiation Engineering, Shahid Beheshti University, Tehran, Iran

## Address for correspondence:

Dr. Iraj Abedi,  
Department of Medical Physics,  
Isfahan University of Medical  
Sciences, Isfahan, Iran.  
E-mail: i.abedi@med.mui.ac.ir

## Access this article online

Website: [www.jmssjournal.net](http://www.jmssjournal.net)

DOI: 10.4103/jmss.JMSS\_83\_20

## Quick Response Code:



are a key element that should be used in image quality assessment. However, its subjective nature greatly contributes to the possible variability of the result. In addition, the data obtained can be difficult to process due to the number of observers involved and the number of images that need to be analyzed. On the other hand, objective method measurements of image data (e.g., signal-to-noise ratio) are not affected by human perception. Consequently, they do not suffer from variations associated with them and are potentially more reliable and reproducible. However, determining the “optimal” image quality can be a complex task because both quantitative metrics (e.g., noise) and the perception of the observer are required.<sup>[9,10]</sup> Therefore, both human and software observers are needed to examine the parameters affecting image quality.

The primary objective of the authors was to direct radiology technician to modify or optimize underlying parameters of the CT scan such as tube current, slice thickness, and reconstruction filter to decrease patient radiation doses and to produce an acceptable image quality for diagnosis.

### Materials and Methods

In this study, routine imaging was considered as a reference for comparing radiation dose and image quality.

#### Scan parameters

At first, the standard-dose head CT protocol was used. Table 1 shows the parameters of scanning. Phantom scanning was then repeated by altering the parameters of scanning. This examination was carried out with a 128-multidetector computed tomography (MDCT) scanner (GE Healthcare. Light Speed VCT). The body mass measurement device (BMMD-7) phantom made in the USA was used to evaluate the image quality.

To study the impact of mA and slice thickness on image quality and the radiation dose, the scan was done with the various mAs and slice thicknesses using a standard filter [Table 2].

Furthermore, to investigate the effect of filter on image quality and radiation dose, the scan was done with the various mAs and slice thicknesses using soft and standard image filters [Table 3].

#### Radiation dose measurement

To demonstrate the average radiation dose that is delivered to the imaged volume, the volume CT dose index (CTDI<sub>vol</sub>) can be utilized for a particular examination.<sup>[11]</sup> Before starting the scan, the CT scan unit was examined using quality control tests. Following each scan, the values of the CTDI<sub>vol</sub> were achieved from the scanned page containing the information about the radiation dose.<sup>[12]</sup>

#### Quantitative image metrics

To analyze the quality of an image, an in-house software was used. To evaluate the performance of the software, we compared its results with the results obtained from observers.

**Table 1: The standard head computed tomography protocol’s scan parameters recommended by the vendor**

Parameters	Amount
Field of view (cm)	25
Collimation	128×0.625
Slice thickness (mm)	2.5
Rotation time (s)	0.5
Pitch	0.4
Tube voltage (KVp)	125
Tube current (mA)	200

**Table 2: Effects of different slice thickness and mA on radiation dose**

	kVp	mA	Filter	Slice thickness (mm)
Basic conditions	120	200	Standard	2.5
Trial conditions	120	200	Standard	5
	120	175	Standard	5
	120	150	Standard	5
	120	125	Standard	5
	120	100	Standard	5
	120	75	Standard	5
	120	50	Standard	5
	120	25	Standard	5

**Table 3: Effects of different image filters on radiation dose**

	kVp	mA	Filter	Slice thickness (mm)
Basic conditions	120	200	Standard	2.5
Trial conditions	120	200	Soft	2.5
	120	175	Soft	2.5
	120	150	Soft	2.5
	120	125	Soft	2.5
	120	100	Soft	2.5
	120	75	Soft	2.5
	120	50	Soft	2.5
	120	25	Soft	2.5

#### Noise measurement

The noise was marked on images of the uniform BMMD-7 CT module as the standard deviation of the pixel values in a square region-of-interest (ROI) situated at the center of the phantom module.

To calculate the level of noise, the size of ROI was 25 × 25 pixels at the center of the image based on the technique explained by Frederic.<sup>[13]</sup> To reduce error and get the proper results, each of the noise values shown in this study was obtained based on eight repetitions of the image, and their average was reported as noise.

#### Noise power spectrum measurement

To carry out an noise power spectrum (NPS) analysis, four 128 × 128-pixel ROIs were derived from each of the reconstructed images. Figure 1 shows that each of the ROIs

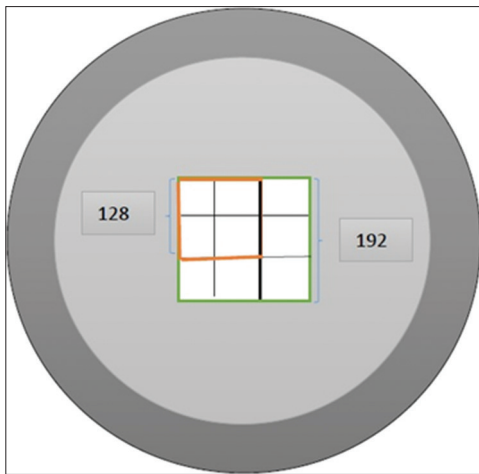


Figure 1: Shows the location of each region of interest in the image

is overlapping its close  $N/2$ -pixel neighbors in vertical and horizontal directions. Sixteen replicated images were used to get a dependable resultant NPS curve, which leads to a collection of 64 ROIs ( $16 \times 4 \times 128 \times 128$  array) employed to calculate each of the NPSs.

Then, the calculation technique, which was suggested by Metheany,<sup>[14]</sup> was utilized as Eq. 1.

$$\text{NPS}(f_x, f_y) = \frac{[FFT_{2D}(f_x, f_y)]^2}{N_{FFT}^2} \Delta l^2 \quad (1)$$

$\Delta p$  represents the size of each of the pixels in the reconstructed image and  $N_{FFT}$  is the number of points employed in fast fourier transforms (FFT) operations.

At first, the total array variance was computed. Next, to exclude the mean value offset prior to using Eq. 1, the mean of pixels in each ROI was calculated and then subtracted from each of the pixels of that ROI. To execute the two-dimensional FFT operation,  $N_{FFT}^2 = (2 \times 128)^2$  points were employed. Furthermore, the size of each pixel in both x and y directions was  $P = 0.4668$ . By placing these values in Eq. 1, the NPS value at each frequency is calculated.

Then calculate the Nyquist frequency by Eq. 2 in both x and y directions of the image and plotted the two-dimensional distribution of NPS in the frequency range  $f$ .

$$f = (1/2 \Delta_p) \quad (2)$$

### High-contrast spatial resolution measurement

The phantom spatial resolution model [Figure 2] consists of seven rows of cavities with a maximum density difference relative to the background. The lowest row in which two adjacent holes are observed separately is considered as the spatial resolution. In other words, a linear array is considered for each row of cavities, and the signal between two cavities varies a lot, two adjacent cavities can be distinguished separately. Therefore, to find the maximum changes, it is necessary to take a derivative in the cavities'

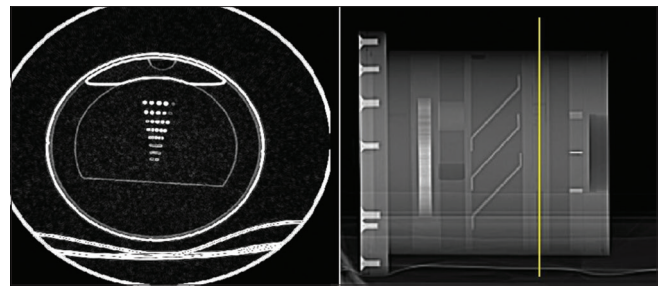


Figure 2: High-contrast spatial resolution calculations

direction. Then, for each array, the differential value was calculated, and its standard deviation was obtained. If the number achieved for each row is greater than the noise threshold, that row is separable. Noise threshold refers to the amount of noise in which adjacent cavities are not distinct. It is repeated for each row to obtain spatial resolution based on a pair of lines per millimeter.

### Low-contrast detectability measurement

A low-contrast BMMD-7 phantom module containing four object groups (e.g., 1%, 3%, 5%, and 6%) with various contrast levels and diameters, as shown in Figure 3. To measure low-contrast detectability (LCD), we planned ROIs on the background and four areas with different densities. Next, the signal of these four object groups was compared with the signal of the background materials. If the difference between the hole signal and the background signal is higher than the threshold value, the hole under consideration can be detected. Accordingly, the number of distinguishable objects was identified for each of the object groups. Here, the value of the threshold is set somewhat more than the image noise.

### Human observer analysis

Three observers analyzed all images obtained in this study in a workstation with constant ambient light and image display contrast. In fact, this task was performed independently by recruiting three board-certified radiologists who specialize in CT scan. The images were randomly provided to observers, and they had no information about the scan parameters associated with each image. Observers could only change the magnification of the images. The images were displayed with a window level of 40 and a width of 80. Each of the three observers investigated a total number of sixty-eight images (34 images of total radiation conditions  $\times$  2 part of the phantom).

### Statistical analysis

SPSS version 23 (SPSS Inc., Chicago, IL, USA) was employed for statistical analysis. To study the correlation between dose, filter, image quality, and slice thickness as latent variables, structural equation modeling (SEM) and linear structural relations were applied. To investigate the relationship between the results, the Spearman rank-order correlation was employed. Furthermore, to evaluate the

relationship between observers, intraclass correlation (ICC) was computed.

## Results

### Qualitative analysis

Table 4 shows high-contrast spatial resolution (HCSR) and LCD qualitative scoring for the three observers. The average ICC was 0.587 with a 95% confidence interval, ranging from 0.261 to 0.871 ( $P < 0.001$ ). HCSR and LCD obtained lower scores to be considered acceptable. Nonetheless, the difference in the score of the average image quality in each of the categories of HCSR and LCD was not statistically significant.

### Noise

According to Figure 4a, increasing the slice thickness at a constant noise reduces the radiation dose. Moreover, using a soft filter instead of a standard filter at a constant noise reduces the radiation dose [Figure 4b].

### Noise power spectrum

FFT techniques were employed to infer NPS from the archived images. The obtained results proposed that ImageJ processing (version 1.51) could be utilized to calculate NPS with confidence. Figure 5 displays NSP curves for 5 mm slice thickness, which were normalized to the curve with 2.5 mm slice thickness. The NPS results indicated almost an identical behavior for 5 mm slice thickness and 125 mA, in comparison with 2.5 mm slice thickness and 200 mA.

As shown in Figure 6, the standard filter curve was used to obtain and normalize NSP curves for the soft filter. The

NPS results for the 100 mA soft filter displayed an identical behavior with the 200 mA standard filter.

### Low-contrast detectability

Figure 7 demonstrates the mean percentage of correct answers given by software readings and human observers for various contrast levels (e.g., 3%, 4%, and 6%) at varying filter (the soft filter rather than the standard filter) and slice thickness. The evaluation of the average results reported by the observer shows that by changing the reconstruction filter and the thickness of the slice, the diagnostic value of the images related to the resolution of objects with different contrasts will not change. In addition, none of the objects with a contrast of 0.5% in the image studied can be distinguished from the background. In general, there was a strong and significant relationship between the value obtained by reading software and the human observer.

### High-contrast spatial resolution

Figure 8 shows the analysis results of high-contrast, spatial resolution, phantom images by software and human observers. According to Figure 8a, as the slice thickness increases, the spatial resolution under different radiation doses was not significantly different from standard radiation conditions ( $P > 0.05$ ). Furthermore, by changing the reconstruction filter, a similar spatial resolution behavior was observed [Figure 8b]. As seen, there was a robust and significant relationship between software readings and human observers ( $\beta = 0.986$ ,  $P = 0.001$ ).

### Structural equation modeling

The conceptual model presented in Figure 9 studies the impact of observed variables on the image quality as a latent variable. According to this model, there was a relatively strong and significant correlation ( $\beta = 0.527$ ,  $P = 0.001$ ) between image quality and the amount of

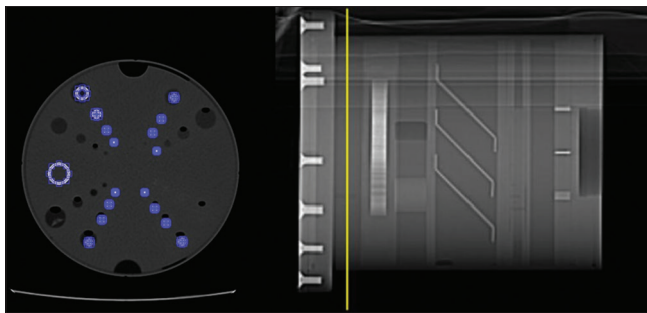


Figure 3: Low-contrast detectability calculations

Table 4: The intraclass correlation values for different parameters

Parameters	ICC	
	High spatial resolution	Low-contrast detectability
Filter	0.261	0.871
Thickness	0.803	0.411

ICC – Intraclass correlation

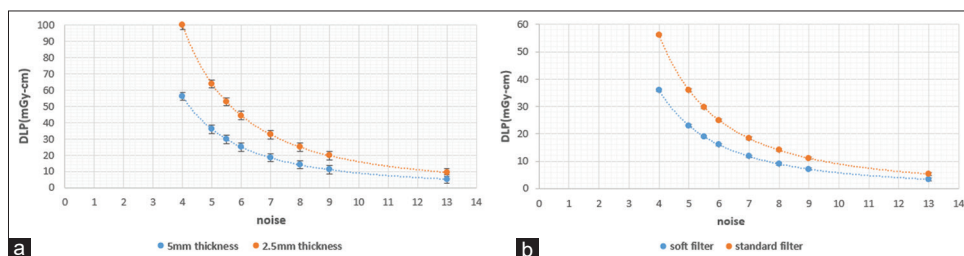


Figure 4: Effect of Slice thickness and filter on radiation dose. (a) Comparison of the radiation dose of different image noise values for 5 and 2.5 mm slice thicknesses. (b) Comparison of the radiation dose of different image noise values for both standard and soft filters



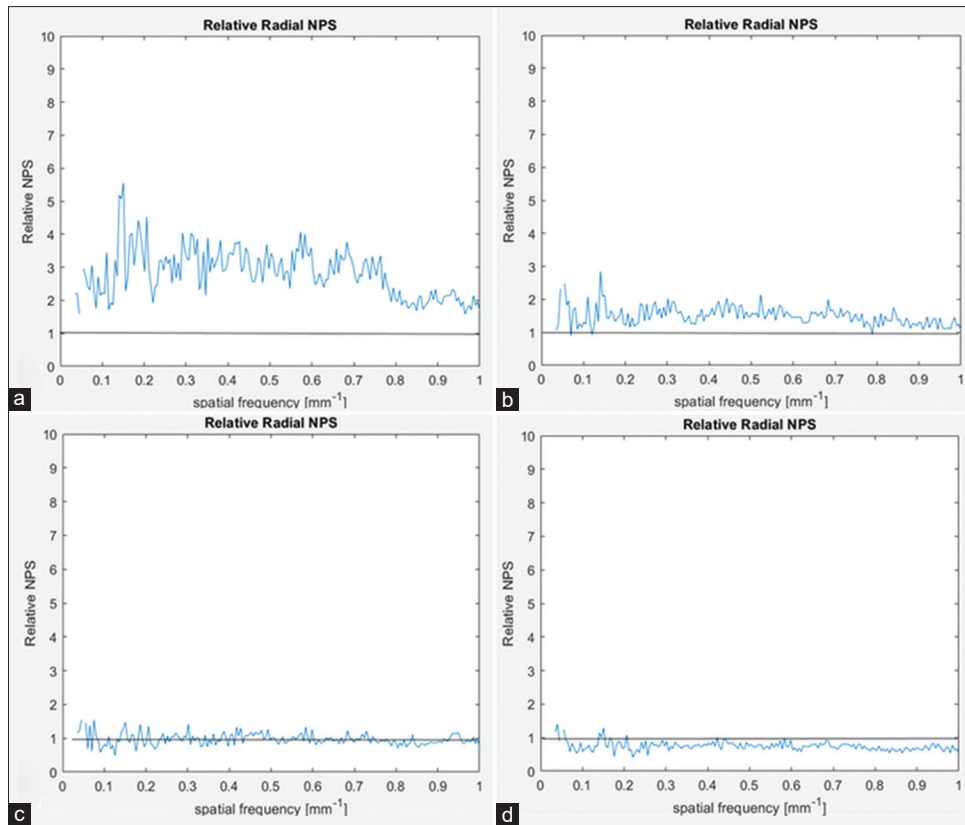


Figure 5: The NPS results for 5 mm slice thickness, normalized to the curve with 2.5 mm with different current tubes. (a) 50 mA, (b) 75 mA, (c) 125 mA, (d) 200 mA. The NPS results indicated almost an identical behavior for 5 mm slice thickness and 125 mA, in comparison with 2.5 mm slice thickness and 200 mA

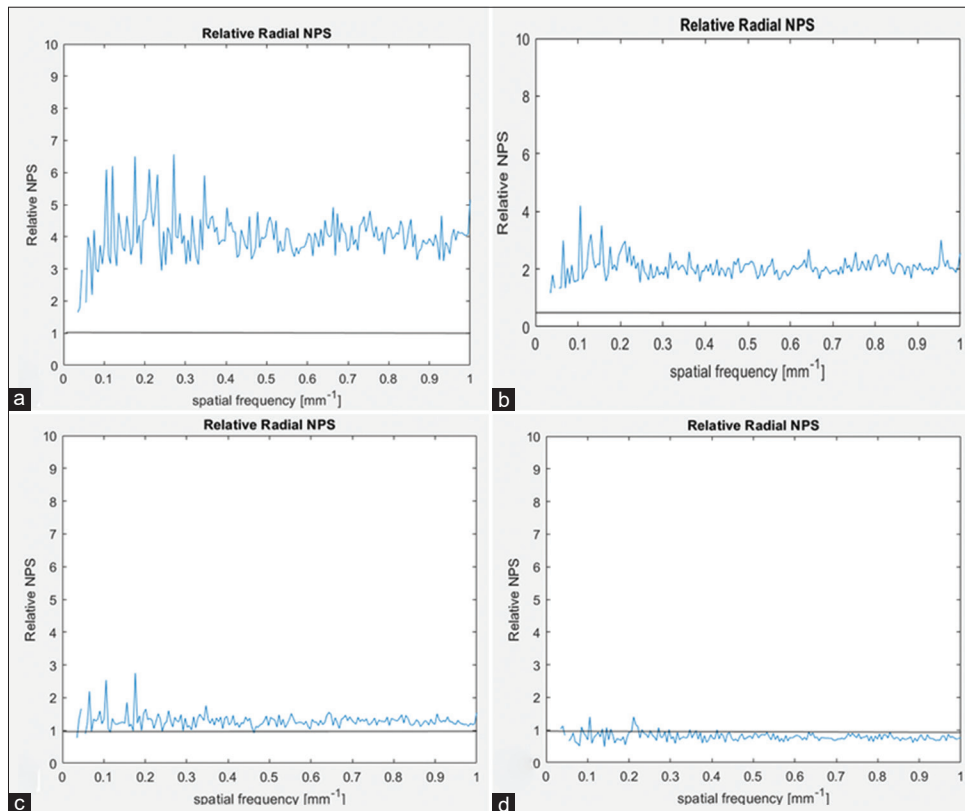


Figure 6: The NPS results for soft filter normalize to standard filter with different current tube. (a) 50 mA, (b) 75, (c) 125 mA, (d) 200 mA. The NPS results for the 100mA soft filter displayed an identical behavior with the 200 mA standard filter

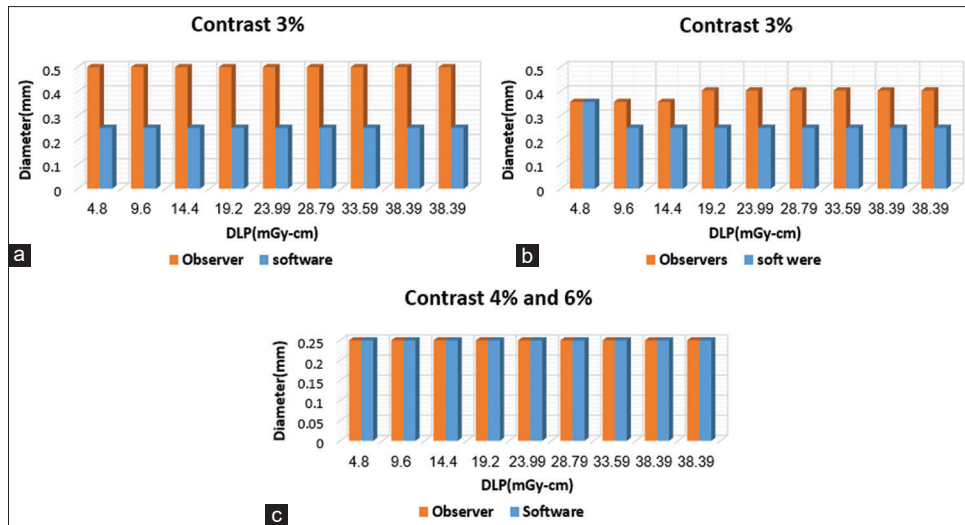


Figure 7: Demonstrate the mean percentage of correct answers given by software readings and human observers for various contrast levels (e.g., 3%, 4%, and 6%) at varying filter (the soft filter rather than the standard filter) and slice thickness. The evaluation of the average results reported by the observer shows that by changing the reconstruction filter and the thickness of the slice, the diagnostic value of the images related to the resolution of objects with different contrasts will not change. the analysis results of high-contrast, spatial resolution, phantom images by software and human observers

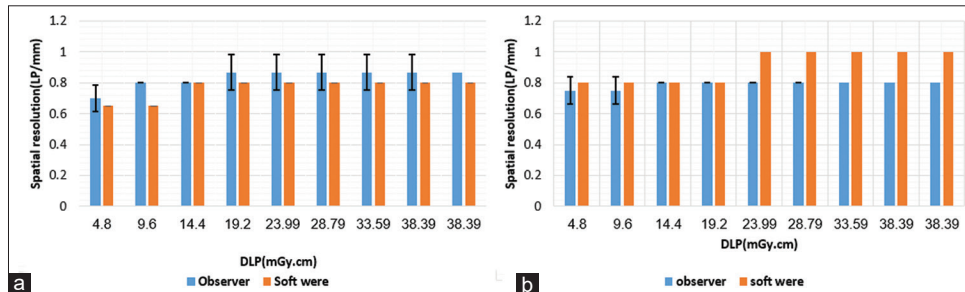


Figure 8: The analysis results of high-contrast, spatial resolution, phantom images by software and human observers

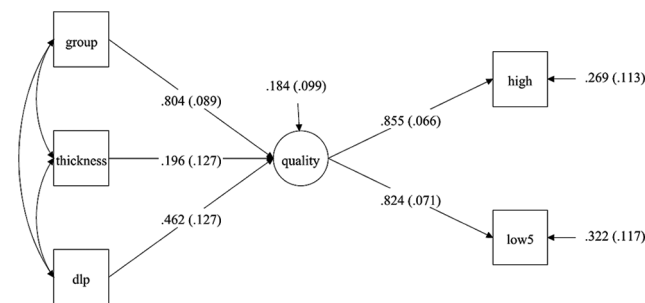


Figure 9: Structural equation modeling models for the relationship between radiation doses with slice thickness. The impact of observed variables on the image quality as a latent variable. As seen, there was a strong and significant correlation between image quality and the amount of radiation

radiation. Furthermore, there is a weak and not statistically significant ( $\beta = 0.164$ ,  $P = 0.001$ ) correlation between slice thickness and image quality. Thus, an increased slice thickness will not contribute to any significant variations in image quality.

In addition, there was a strong and significant relationship ( $\beta = 0.986$ ,  $P = 0.001$ ) between software readings and human observers (as a group (and image quality. That is, the image analysis accuracy has significantly increased

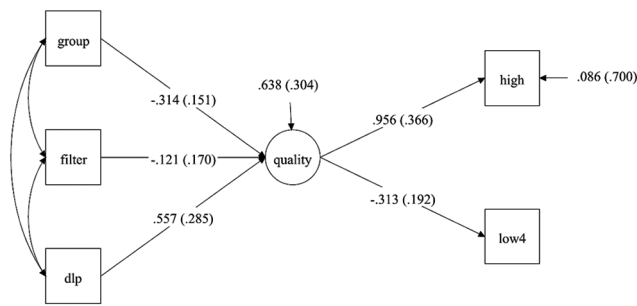
by transforming the reader from the human observer to software.

Figure 10 displays SEM model for the impact of filter on image quality. According to this model, there was a relatively strong and significant correlation ( $\beta = 0.557$ ,  $P = 0.049$ ) between the amount of radiation with image quality. Moreover, there is a negative and not statistically significant correlation between the filter and image quality ( $\beta = -0.121$ ,  $P = 0.474$ ). Therefore, a slight increase in image quality is mediated by using a soft filter rather than a standard filter. The reason why the filter has a weak impact on image quality is that we have regarded low contrast and spatial resolution as the only two constructive parameters in the conceptual model.

Furthermore, there was a strong and significant relationship ( $\beta = -0.314$ ,  $P = 0.038$ ) between software readings and human observers (as a group (and image quality. The reason why the beta is negative is the read error (i.e. bias) by an observer, leading observers enhance image quality in comparison with software.

## Discussion

Radiation dose is closely related to image quality; hence, increasing the radiation dose can help improve image



**Figure 10: Structural equation modeling models for the relationship between radiation doses with reconstruction filter. The impact of filter on image quality. As seen, there was a strong and significant correlation between the amounts of radiation with image quality**

quality. To obtain a definitive and accurate diagnosis, it is very important to reduce the radiation dose and maintain high-quality diagnostic images. According to existing documents,<sup>[15-17]</sup> patient doses are higher than normal, and CT image quality usually exceeds the level required for confident diagnosis. However, according to the results of our study, the radiation dose can be reduced by 30%–50% by increasing the slice thickness and using soft filters instead of standard filters.

The majority of previous studies on dose reduction used postprocessing or iterative reconstruction (IR) algorithms in the shape of nonlinear filters.<sup>[14,18,19]</sup> Nevertheless, the IR techniques are a bit slower in terms of reconstruction time and are available on advanced scanners (i.e., 64 cuts or higher), CT scanners with a substantial increase in cost for both software and hardware upgrades. Accordingly, optimization of scan protocols such as slice thickness and reconstruction filter is very important to reduce the radiation dose. In this study, we demonstrated that increasing the slice thickness by 2.5 units leads to reduce the radiation dose by 30%–50% units without changing the spatial resolution, NPS and LCD. This finding is consistent with the Tamm study,<sup>[20]</sup> which can prevent higher radiation doses caused by CT examinations while maintaining sufficient image quality by modifying the scan parameters. In another study by Pierre D *et al.*, the effects of key operator-chosen CT parameters on patient radiation dose were evaluated. According to this study, depending on the slice thickness required for a diagnostic study, the mAs, kVp, or both may need to be increased to offset the increased noise from the thinner sections. On the other hand, the radiation dose must change in inverse proportion to the slice thickness to maintain constant image noise for varying reconstructed slice thicknesses.<sup>[6]</sup> In addition, Kalpana *et al.* showed that the noise index change from 40 to 30 at a fixed slice thickness of 0.625 mm increases the radiation dose by 80%.<sup>[7]</sup>

Moreover, the present study results showed that the reconstruction filter generally is essential tool in image quality. The soft filter contributes to a reduction in noise

by compromising spatial resolution, while the standard filter contributes to an improvement in spatial resolution by the increased noise.<sup>[21]</sup> Our study also demonstrated that changing the reconstruction filter can reduce the radiation dose by up to 50%.

Typically, for each medical application, the most appropriate slice thickness and reconstruction filter should be selected to reduce the radiation dose according to the required image quality.

As well, we designed and implemented a modern comparative analysis method (SEM analysis) in relation to radiation dose and image quality using software- and observer-based evaluations to modify the parameters of the CT scan. The SEM analysis is used to analyze structural relationships. This technique is the combination of factor analysis and multiple regression analysis, and it is used to analyze the structural relationship between measured (slice thickness, reconstruction filter, and radiation dose) variables and latent (image quality) constructs.

The results consistently indicate that SEM model-driven approaches were as effective as observer-based approaches.

Our study had a number of limitations, including the fact that only the scanning parameters of the scanner model were evaluated. In addition, no clinical evaluation was performed, only physical parameters that affect image quality were examined. This study needs to be completed with a clinical evaluation.

### Conclusion

In this study, it was shown that in the brain CT scan imaging, the radiation dose was reduced by 30%–50% by increasing the slice thickness or changing the reconstruction filter. It is necessary to adjust the CT scan protocols according to clinical requirements or the special conditions of some patients while maintaining acceptable image quality.

### Acknowledgments

The authors gratefully acknowledge financial support from the Isfahan University of Medical Science (IUMS) (grant No. 297172). In addition, we would like to thank those who have provided valuable suggestions, or who have contributed to the manuscript.

### Financial support and sponsorship

None.

### Conflicts of interest

There are no conflicts of interest.

### References

1. McCollough CH, Chen GH, Kalender W, Leng S, Samei E, Taguchi K, *et al.* Achieving routine submillisievert CT scanning: Report from the summit on management of radiation dose in CT.

- Radiology 2012;264:567-80.
2. Boone JM, Hendee WR, McNitt-Gray MF, Seltzer SE. Radiation exposure from CT scans: How to close our knowledge gaps, monitor and safeguard exposure – Proceedings and recommendations of the radiation dose summit, sponsored by NIBIB, February 24-25, 2011. Radiology 2012;265:544-54.
  3. Patro SN, Chakraborty S, Sheikh A. The use of adaptive statistical iterative reconstruction (ASiR) technique in evaluation of patients with cervical spine trauma: Impact on radiation dose reduction and image quality. Br J Radiol 2016;89:20150082.
  4. Brenner DJ, Hall EJ. Computed tomography — An increasing source of radiation exposure. N Engl J Med 2007;357:2277-84.
  5. Imhof H, Schibany N, Ba-Ssalamah A, Czerny C, Hojreh A, Kainberger F, *et al.* Spiral CT and radiation dose. Eur J Radiol 2003;47:29-37.
  6. Raman SP, Mahesh M, Blasko RV, Fishman EK. CT scan parameters and radiation dose: Practical advice for radiologists. J Am Coll Radiol 2013;10:840-6.
  7. Kanal KM, Stewart BK, Kolokythas O, Shuman WP. Impact of operator-selected image noise index and reconstruction slice thickness on patient radiation dose in 64-MDCT. AJR Am J Roentgenol 2007;189:219-25.
  8. Paul J, Krauss B, Banckwitz R, Maentele W, Bauer RW, Vogl TJ. Relationships of clinical protocols and reconstruction kernels with image quality and radiation dose in a 128-slice CT scanner: Study with an anthropomorphic and water phantom. Eur J Radiol 2012;81:e699-703.
  9. Cohen G, McDaniel DL, Wagner LK. Analysis of variations in contrast-detail experiments. Med Phys 1984;11:469-73.
  10. Swensson RG, Judy PF. Detection of noisy visual targets: Models for the effects of spatial uncertainty and signal-to-noise ratio. Percept Psychophys 1981;29:521-34.
  11. Céliér D, Roch P, Etard C, Le Pointe HD, Brisse HJ. Multicentre survey on patient dose in paediatric imaging and proposal for updated diagnostic reference levels in France. Part 1: Computed tomography. Eur Radiol 2020;30:1156-65.
  12. Meeson S, Turnbull SD, Patel R, Golding SJ. Initial radiation dose reduction studies in cervical spine multidetector CT. Biomedical Physics & Engineering Express. 2018;4:025005.
  13. Shah SM, Deep K, Siramanakul C, Mahajan V, Picard F, Allen DJ. Computer navigation helps reduce the incidence of noise after ceramic-on-ceramic total hip arthroplasty. J Arthroplasty 2017;32:2783-7.
  14. Shaqdan KW, Kambadakone AR, Hahn P, Sahani DV. Experience with iterative reconstruction techniques for abdominopelvic computed tomography in morbidly and super obese patients. J Comput Assist Tomogr 2018;42:124-32.
  15. Kanal KM, Butler PF, Sengupta D, Bhargavan-Chatfield M, Coombs LP, Morin RL. U.S. diagnostic reference levels and achievable doses for 10 adult CT examinations. Radiology 2017;284:120-33.
  16. Kim Y, Kim YK, Lee BE, Lee SJ, Ryu YJ, Lee JH, *et al.* Ultra-low-dose ct of the thorax using iterative reconstruction: Evaluation of image quality and radiation dose reduction. AJR Am J Roentgenol 2015;204:1197-202.
  17. Goo HW. Is it better to enter a volume CT dose index value before or after scan range adjustment for radiation dose optimization of pediatric cardiothoracic CT with tube Current modulation? Korean J Radiol 2018;19:692-703.
  18. Yan C, Xu J, Liang C, Wei Q, Wu Y, Xiong W, *et al.* Radiation dose reduction by using CT with iterative model reconstruction in patients with pulmonary invasive fungal infection. Radiology 2018;288:285-92.
  19. Maruyama S, Fukushima Y, Miyamae Y, Koizumi K. Usefulness of model-based iterative reconstruction in semi-automatic volumetry for ground-glass nodules at ultra-low-dose CT: A phantom study. Radiol Phys Technol 2018;11:235-41.
  20. Tamm EP, Rong XJ, Cody DD, Ernst RD, Fitzgerald NE, Kundra V. Quality initiatives: CT radiation dose reduction: How to implement change without sacrificing diagnostic quality. Radiographics 2011;31:1823-32.
  21. Deloire L, Diallo I, Cadieu R, Auffret M, Alavi Z, Ognard J, *et al.* Post-mortem X-ray computed tomography (PMCT) identification using ante-mortem CT-scan of the sphenoid sinus. J Neuroradiol 2019;46:248-55.